Journal of Sound and Vibration (2001) **239**(4), 801–817
doi:10.1006/jsvi.2000.3129, available online at http://www.idealibrary.com on IDEAL®

ON THE HYDROACOUSTICS OF A TRAILING EDGE WITH A DETACHED FLAP

M. S. Howe

Department of Aerospace and Mechanical Engineering, Boston University, College of Engineering, 110 Cummington Street, Boston, MA 02215, *U.S.A.*

(*Accepted* 2 *May* 2000)

An analysis is made of production of sound by low Mach number turbulent flow over the trailing edge of a hydrofoil with a single detached flap. Following the approach advocated by Professor Doak in 1960 (Proceedings of the Royal Society A **254**, 129–145), an aeroacoustic Green function is derived for a hydrofoil of large chord with a detached flap at relative angle of attack α ($\alpha^2 \ll 1$) when the chord of the flap is acoustically compact. The Green function can be used with data derived from direct numerical simulations of the unsteady hydrodynamic flow, and provides an effective means of calculating the radiation from a knowledge of the *incompressible* component of the flow in the edge region. The results permit a comparison to be made of the separate contributions to the production of sound by turbulence interacting with the trailing edge of the hydrofoil, the trailing edge of the flap, and with the leading edge of the flap. The side-edge noise of part-span flaps is not discussed. Formulae are given for calculating the "self-noise" produced at trailing edges by boundary layer instability; the efficiency of sound generation at the edge of the hydrofoil is shown to be typically at least 7 dB larger than that produced at the trailing edge of the flap. The impingement noise generated by small-scale turbulence interacting with the flap leading edge is expressed in terms of an equivalent dipole source equal to the fluctuating flap-lift force, acting at a distance l_F to the rear of the main hydrofoil; l_F is determined as a function of the flap dimensions, and does not normally exceed about twice the width h of the slot separating the hydrofoil and flap. The proximity of the dipole to the edge of the hydrofoil increases the efficiency of sound production by a factor proportional to $h/(l_F M)$ where $M \ll 1$ is the characteristic edge flow Mach number, and modifies the directivity of the sound.

1. INTRODUCTION

The efficiency with which sound is generated by very low Mach number "hydroacoustic" flows is so small that the unsteady motion in the source region is effectively indistinguishable from that of an incompressible fluid. Great caution must therefore be exercised in interpreting numerical predictions of the minute acoustic byproduct of the flow, and it is unwise to invest too much confidence in direct numerical simulations of sound production, which are often dominated by numerical rather than acoustic noise. It is particularly difficult, for example, to make reliable estimates of the sound produced by turbulence in the neighborhood of a solid surface whose radius of curvature is large relative to the acoustic wavelength. Both the amplitude and directionality of the sound are crucially dependent on the relative phasing of very small source components distributed over surface regions spanned by many acoustic wavelengths; such phase variations are largely indeterminate by conventional numerical procedures when the flow is effectively incompressible, and spurious noise predictions can result from the indiscriminate use of

0022-460X/01/040801 + 17 $35.00/0

computed data in, say, Curle's [1] or Kirchhoff's [2] surface integral representation of the sound.

This paper is concerned with the important special case of the generation of sound by low Mach number turbulent flow in the vicinity of the trailing edge of a hydrofoil whose chord is generally large relative to the acoustic wavelength. Numerical predictions in which Curle's equation [1] (or the Ffowcs Williams–Hawkings equation [3]) is used with hydrofoil surface data derived from an incompressible numerical simulation of the flow are known to be incorrect [4, 5]. Theoretical methods for studying this problem are usually based on "diffraction theory" [2, 6–8], according to which sound is produced when the hydrodynamic pressure field of turbulence is swept over the edge in the mean flow and diffracted by the edge, or on Lighthill's acoustic analogy theory used in conjunction with a *compact* Green function tailored to the trailing edge geometry [2, 9–11], in the manner proposed by Doak [12]. These methods are equivalent at low Mach numbers; their advantage is that they unambiguously identify fluid–structure interactions at the trailing edge as the source of sound, as opposed to locations on the extensive, near planar hydrofoil surface upstream of the edge, where a numerical simulation of the predominantly incompressible flow would supply no information about source phasing. In other words, as with the original application of Lighthill's theory to free-field turbulence quadrupole sources, both of these theoretical approaches provide estimates of the edge noise from a knowledge of the *incompressible* characteristics of the flow near the edge.

Numerical predictions of trailing edge noise that are consistent with measurements have been made by Wang [13, 14] and Wang and Moin [15] by combining the results of direct numerical simulations of incompressible trailing edge flows with an integral representation of the sound involving the compact Green function. These calculations have hitherto treated the acoustic problem in terms of the Green function for a trailing edge modelled by a semi-infinite rigid plate [9], but the method of conformal transformation permits more general edge geometries to be considered, including hydrofoils of finite thickness [2, 5] and finite chord [16].

An important special case arises for a trailing edge with a detached "flap" [17–19] (or with the deployment of a leading edge "slat" [20]). Noise is generated at the side-edges of part-span flaps and also within the spanwise slot between the hydrofoil and flap. At very low Mach numbers, typical of those encountered in underwater applications, a compact Green function can be constructed for dealing with the production of sound by side-edge sources [21, 22]. Howe [23, 24] has discussed simplified *two-dimensional* analytical models of the influence of the slot between the deployed flap and the hydrofoil; in reference [23] the flap chord was assumed to be large compared to the acoustic wavelength; in reference [24] a vortex sheet model for the unsteady flow in the slot was postulated.

However, to derive reliable analytical predictions of the intensities of noise produced by general, three-dimensional hydroacoustic source distributions in the vicinity of the slot, it is necessary that the Green function take explicit account of the doubly connected trailing edge geometry. The radiated sound can then be calculated from measurements or from numerical simulations of the unsteady hydrodynamic flow in the slot. In this paper, a formula is developed for the compact Green function for a flap of large aspect ratio in the limit of the very small mean flow Mach numbers typical of underwater applications, when the chord of the flap may be regarded as small compared to the acoustic wavelength. In the first instance, this is done by modelling the hydrofoil by a semi-infinite rigid plate with a detached flap in the form of a rigid strip at a small angle of attack to the hydrofoil. When the turbulence scales are small relative to the slot width, the leading and trailing edges of the slot and the trailing edge of the flap may be identified as sources of sound whose relative importance can be estimated from the functional form of the Green function. These

conclusions can also be applied to a hydrofoil and flap of finite thickness and rounded edge geometry, provided the slot width is large compared to the thickness of the flap near its leading edge. Similarly, a correction can be introduced in the manner described in reference [16] to take account of the finite chord of the hydrofoil.

The general representation of sound produced at low Mach numbers by fluid–structure interactions is recalled in section 2. The Green function for a flap at small angle of attack is derived in section 3, and approximations are obtained for its behavior near the edges of the flap and hydrofoil. The special but important case in which the length scales of the dominant turbulence sources are small compared to the chord of the flap is discussed in section 4, where the radiation efficiencies of the different edges are investigated, and where leading edge, flap-impingement noise is identified as the most important source in the slot. It is shown for this case how the noise can be represented in terms of an equivalent dipole source (whose strength is equal to the unsteady lift on the flap) placed at a suitable position to the rear of the hydrofoil.

2. FORMULATION OF THE PROBLEM

2.1. TRAILING EDGE NOISE

Consider the generation of sound at low Mach numbers by turbulent flow in the vicinity of the trailing edge of a hydrofoil. It is first assumed that the trailing edge region has the idealized form illustrated in Figure 1. The hydrofoil is at rest within a mean stream at speed U in the positive x_1 direction of the rectangular co-ordinate system (x_1, x_2, x_3), and is modelled by a semi-infinite rigid plate occupying the half-plane $x_1 < 0, x_2 = 0$; the detached "flap" consists of a uniform, rigid strip of width l inclined at angle α to the hydrofoil. The slot separating the hydrofoil and the leading edge of the flap has width h. The objective is to determine the influence of the flap and slot on the generation of aerodynamic sound, but no account will be taken of the side-edges of part span flaps.

Let $\mathbf{v}$ and $\boldsymbol{\Omega} = \text{curl } \mathbf{v}$, respectively, denote the velocity and vorticity, and let c_0 be the speed of sound. When the mean flow Mach number $M = U/c_0 \ll 1$ the convection of sound by the mean flow may be neglected, and the aerodynamically generated sound is determined by the solution of

$$\left(\frac{1}{c_0^2}\frac{\partial^2}{\partial t^2} - \nabla^2\right) B = \text{div}\,(\boldsymbol{\Omega} \wedge \mathbf{v}), \tag{1}$$

where t denotes time and B is the total enthalpy [2, 5]. In the acoustic far field (at large distances from the source region) the pressure $p(\mathbf{x}, t) = \rho_0 B(\mathbf{x}, t)$, where ρ_0 is the mean fluid density. By making use of the momentum equation in the form

$$\partial \mathbf{v}/\partial t + \nabla B = -\boldsymbol{\Omega} \wedge \mathbf{v} - \nu \,\text{curl}\,\boldsymbol{\Omega} \quad (\nu = \text{kinematic viscosity}),$$

and writing $p(\mathbf{x}, t) = \int_{-\infty}^{\infty} p(\mathbf{x}, \omega)\, e^{-i\omega t}\, d\omega$, the pressure in the acoustic far field can be written [2, 5]

$$\frac{p(\mathbf{x}, \omega)}{\rho_0} = \int \frac{\partial G}{\partial \mathbf{y}}(\mathbf{x}, \mathbf{y}, \omega) \cdot (\boldsymbol{\Omega} \wedge \mathbf{v})(\mathbf{y}, \omega)\, d^3\mathbf{y} - \nu \oint_S \boldsymbol{\Omega}(\mathbf{y}, \omega) \wedge \frac{\partial G}{\partial \mathbf{y}}(\mathbf{x}, \mathbf{y}, \omega) \cdot \mathbf{n}\, dS(\mathbf{y}) \quad |\mathbf{x}| \to \infty, \tag{2}$$

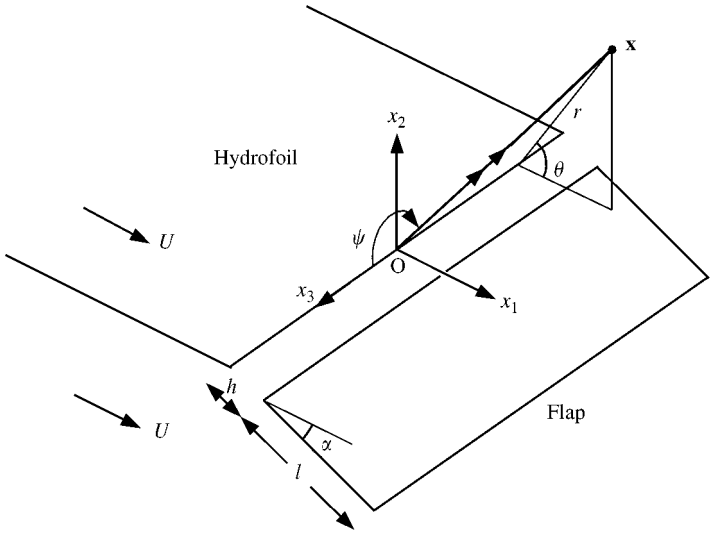

Figure 1. Idealized hydrofoil and flap, illustrating the angles θ and ψ defining the point $\mathbf{x}$ in the acoustic far field.

where the second integral is taken over the surface S of the hydrofoil and flap, $\mathbf{n}$ being the surface normal directed into the fluid. $G(\mathbf{x}, \mathbf{y}; \omega)$ is the *time harmonic* acoustic Green function (having outgoing wave behavior), which satisfies

$$(\nabla^2 + \kappa_0^2)G = \delta(\mathbf{x} - \mathbf{y}), \quad \kappa_0 = \omega/c_0\,, \tag{3}$$

and has vanishing normal derivatives $\partial G(\mathbf{x}, \mathbf{y}; \omega)/\partial x_n = 0$, $\partial G(\mathbf{x}, \mathbf{y}; \omega)/\partial y_n = 0$, respectively, for $\mathbf{x}$ and $\mathbf{y}$ on S. When $M \ll 1$ the acoustic pressure is determined to an excellent approximation by equation (2) by approximating $\mathbf{v}$ and $\boldsymbol{\Omega}$ in the integrands by their values for the incompressible flow [2]. Both integrals correspond to distributions of acoustic sources of dipole type, and, respectively, represent contributions produced by the normal and frictional stresses exerted on S. At high Reynolds number the frictional component can be neglected.

The sound can also be represented entirely as a surface integral over S by introducing the upwash velocity $\mathbf{v}_\mathrm{I}$, defined by the Biot–Savart formula [25, 26]

$$\mathbf{v}_\mathrm{I}(\mathbf{x}, t) = \mathrm{curl} \int \frac{\boldsymbol{\Omega}(\mathbf{y}, t)\,\mathrm{d}^3\mathbf{y}}{4\pi|\mathbf{x} - \mathbf{y}|}, \tag{4}$$

where the integration is confined to the fluid (i.e., *bound* vorticity on the hydrofoil is excluded). This is the velocity field induced by the vorticity when the presence of the hydrofoil is temporarily ignored (although its presence must be taken into account when determining $\boldsymbol{\Omega}$). The velocity is "scattered" by S, and the resulting sound can be expressed in the form [5]

$$\frac{p(\mathbf{x}, \omega)}{\rho_0} = \oint_S \left(-\mathrm{i}\omega \mathbf{v}_I(\mathbf{y}, \omega) G(\mathbf{x}, \mathbf{y}, \omega) - \nu \boldsymbol{\Omega}(\mathbf{y}, \omega) \wedge \frac{\partial G}{\partial \mathbf{y}}(\mathbf{x}, \mathbf{y}, \omega) \right) \cdot \mathbf{n}\,\mathrm{d}S(\mathbf{y}), \quad |\mathbf{x}| \to \infty. \tag{5}$$

To use this formula a preliminary calculation would need to be performed to determine the unsteady vorticity distribution $\mathbf{\Omega}$ close to the hydrofoil. The velocity $\mathbf{v}_I$ is then calculated from equation (4); it is precisely the "kinematic" velocity induced by the vortex field $\mathbf{\Omega}$ when the influence of "image" vortices within S (i.e., the influence of *scattering* by S) is ignored.

Equations (2) and (5) give alternative, but equivalent representations of the sound in terms of the same Green function $G(\mathbf{x}, \mathbf{y}, \omega)$ that has a vanishing normal derivative on S. The choice of which formulation to use will in practice depend on the details of the problem at hand.

2.2. ACOUSTICALLY COMPACT FLAP

Trailing edge interaction noise is determined by the contributions to the integrals in equation (2) from the neighborhood of the edge region. The wavelength of the sound $\sim \delta/M$, where δ is the turbulence eddy length scale near the edge, and can be expected to exceed the flap chord l when $M \ll 1$ (in water, for example, M is not normally larger than about 10^{-2}). The unsteady flow structures that generate edge noise are then very much closer than an acoustic wavelength ($\sim 1/\kappa_0$) from the trailing edge region. This means that the non-dimensional source distance $\kappa_0 \sqrt{y_1^2 + y_2^2} \ll 1$, and the Green function may accordingly be expanded in powers of this parameter. The leading terms in the expansion when the observation point $\mathbf{x}$ lies in the acoustic far field are [2]

$$G(\mathbf{x}, \mathbf{y}, \omega) = G_0(\mathbf{x}, \mathbf{y}, \omega) + G_1(\mathbf{x}, \mathbf{y}, \omega) + \cdots \quad |\mathbf{x} - y_3\mathbf{i}_3| \to \infty, \tag{6}$$

where $\mathbf{i}_3$ is a unit vector in the spanwise (x_3) direction, and

$$G_0(\mathbf{x}, \mathbf{y}, \omega) = \frac{-\mathrm{e}^{\mathrm{i}\kappa_0|\mathbf{x} - y_3\mathbf{i}_3|}}{4\pi|\mathbf{x} - y_3\mathbf{i}_3|}, \quad G_1(\mathbf{x}, \mathbf{y}, \omega) = \frac{-\sqrt{\kappa_0}\sin^{1/2}\psi \sin(\theta/2)\varphi^*(\mathbf{y})\mathrm{e}^{\mathrm{i}\kappa_0|\mathbf{x} - y_3\mathbf{i}_3|}}{\pi\sqrt{2\pi\mathrm{i}}|\mathbf{x} - y_3\mathbf{i}_3|}. \tag{7}$$

If $r = \sqrt{x_1^2 + x_2^2}$, the shortest distance of $\mathbf{x}$ from the edge of the hydrofoil (the x_3-axis), then $\psi = \sin^{-1}(r/|\mathbf{x}|)$ is the angle shown in Figure 1 between the direction of $\mathbf{x}$ and the edge, and (r, θ) are the polar co-ordinates of $\mathbf{x}$ in a plane $x_3 = \text{constant}$, so that $(x_1, x_2) = r(\cos\theta, \sin\theta)$. The function $\varphi^*(\mathbf{y}) \equiv \varphi^*(y_1, y_2)$ of the source position $\mathbf{y}$ satisfies Laplace's equation, and has the simple interpretation as a velocity potential of ideal, incompressible flow in the anticlockwise direction in the figure around the edge, with zero circulation about the flap. It is normalized by the requirement that

$$\varphi^*(\mathbf{y}) \to \bar{\varphi}^*(\mathbf{y}) \equiv \sqrt{r'}\sin(\theta'/2) \text{ as } r' \to \infty, \text{ where } (y_1, y_2) = r'(\cos\theta' \sin\theta'), \tag{8}$$

where $\bar{\varphi}^*(\mathbf{y})$ is the velocity potential of flow around the rigid *half-plane* $x_1 < 0$, $x_2 = 0$ [25, 26]. The presence of these potential functions can be understood as follows: The reciprocal theorem permits the behavior of $G(\mathbf{x}, \mathbf{y}, \omega)$ as a function of $\mathbf{y}$ near the edge to be computed by considering the diffraction problem in which a point source is placed at the point $\mathbf{x}$ in the acoustic far field. The motion induced by this source at distances from the flap that are smaller than an acoustic wavelength may then be seen to correspond to an ideal, incompressible edge flow with velocity potential proportional to $\varphi^*(\mathbf{y})$.

The zeroth order component G_0 in expansion (6) has the same structure as the free-space acoustic Green function, and when used in equation (2) or equation (5) yields contributions to the acoustic pressure that are equivalent to the sound generated by free-field turbulence

quadrupoles. The main contribution to the radiation (whose amplitude is larger by a factor $\sim 1/M^{3/2} \gg 1$ than that produced by the quadrupoles) is generated by "edge scattering" and is governed in a first approximation by the second term G_1 in equation (6). In the high Reynolds number limit, when surface shear stresses are small relative to the normal surface stresses, equations (2) and (5) therefore yield the following alternative, leading order representations:

$$p(\mathbf{x}, \omega) \approx \frac{-\rho_0 \kappa_0^{1/2} \sin^{1/2}\psi \sin(\theta/2)}{\pi\sqrt{2\pi \mathrm{i}}\,|\mathbf{x}|} \int \frac{\partial \varphi^*(\mathbf{y})}{\partial \mathbf{y}} \cdot (\boldsymbol{\Omega} \wedge \mathbf{v})(\mathbf{y}, \omega) \mathrm{e}^{\mathrm{i}\kappa_0 |\mathbf{x} - \mathrm{i}y_3 \mathbf{i}_3|}\, \mathrm{d}^3 \mathbf{y}$$

$$= \frac{\rho_0\, \omega \sqrt{\mathrm{i}\kappa_0} \sin^{1/2}\psi \sin(\theta/2)}{\pi\sqrt{2\pi}\,|\mathbf{x}|} \oint_S \varphi^*(\mathbf{y}) v_{1n}(\mathbf{y}, \omega)\, \mathrm{e}^{\mathrm{i}\kappa_0 |\mathbf{x} - \mathrm{i}y_3 \mathbf{i}_3|}\, \mathrm{d}S(\mathbf{y}), \quad |\mathbf{x}| \to \infty, \tag{9}$$

where $v_{In} = \mathbf{v}_I \cdot \mathbf{n}$.

3. GREEN'S FUNCTION

3.1. CALCULATION OF φ^*

The function $\varphi^*(\mathbf{y}) \equiv \varphi^*(y_1, y_2)$ is equivalent to the velocity potential of two-dimensional, incompressible flow around the trailing edge region of the hydrofoil, and may be determined by the method of conformal transformation [25, 26]. In the thin-plate approximation, the hydrofoil occupies the negative real axis in the plane of $z = y_1 + \mathrm{i}y_2$; the flap lies along the ray $\arg z = -\alpha$ between $z = h\mathrm{e}^{-\mathrm{i}\alpha}$ and $z = H\mathrm{e}^{-\mathrm{i}\alpha}$, where $H = l + h$ (see Figure 2(a)).

The transformation

$$\zeta = \sqrt{z/h} \tag{10}$$

maps the fluid region bounded by the hydrofoil and flap onto the right half of the ζ-plane, with the "upper" and "lower" sides ($\mathrm{A}_\infty\mathrm{O}$ and $\mathrm{B}_\infty\mathrm{O}$, respectively), of the hydrofoil mapping onto the imaginary axis, as indicated in Figure 2(b). The flap maps into the interval $\zeta = \mathrm{e}^{-\mathrm{i}\varepsilon}$ to $\zeta = \mathrm{e}^{-\mathrm{i}\varepsilon}/\sqrt{m}$ of the ray $\arg \zeta = -\varepsilon$, where $\varepsilon = \alpha/2$ and $m = h/H$.

Irrotational flow in the anticlockwise sense around the trailing edge region in the z-plane corresponds to flow past the flap in the ζ-plane from $\zeta = -\mathrm{i}\infty$ to $\zeta = +\mathrm{i}\infty$ that becomes parallel to the imaginary axis as $|\zeta| \to \infty$. We can write

$$\varphi^*(\mathbf{y}) = \mathrm{Re}\, w(\zeta), \tag{11}$$

where $w(\zeta)$ is the complex potential of the flow in the ζ-plane. The potential can be calculated in closed form when $\varepsilon = \alpha/2 = 0$; the solution for $\varepsilon \neq 0$ is found by iteration, by writing

$$w(\zeta) = w_0(\zeta) + \varepsilon w_1(\zeta) + \cdots, \text{ i.e., } \varphi^*(\mathbf{y}) = \varphi_0^*(\mathbf{y}) + \varepsilon\varphi_1^*(\mathbf{y}) + \cdots. \tag{12}$$

The zeroth order problem for $w_0(\zeta)$ is illustrated in Figure 2(c). The flap lies along the real axis between $\zeta = 1, 1/\sqrt{m}$; the imaginary axis forms a rigid barrier that may be removed by

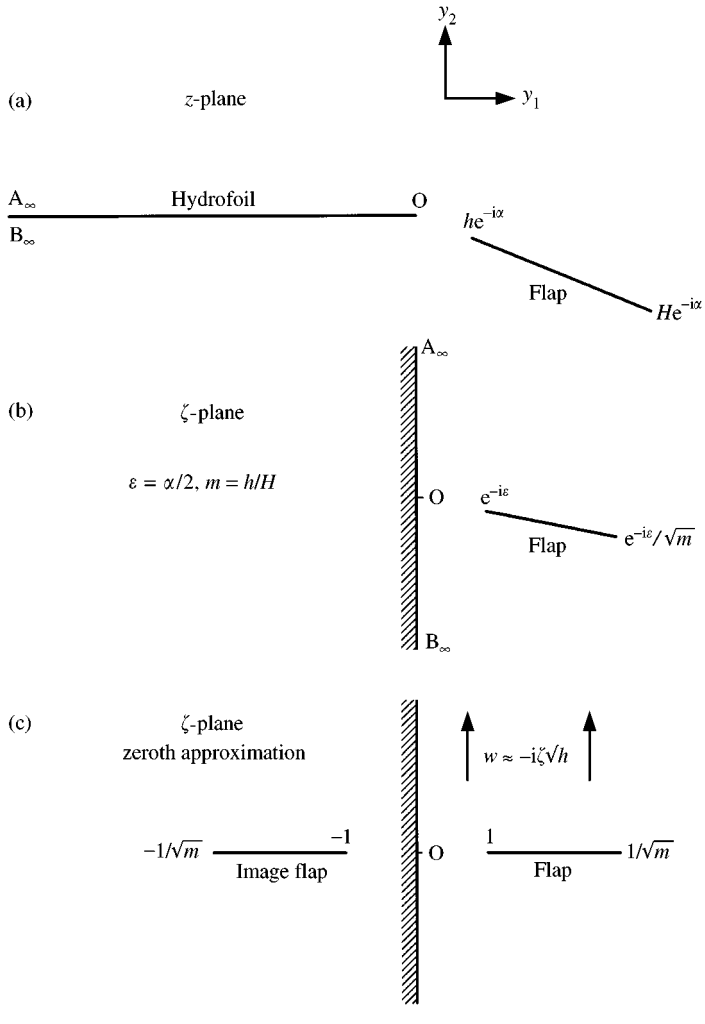

Figure 2. (a) Thin plate hydrofoil and flap in the z-plane; (b) image in the ζ-plane; (c) configuration in the ζ-plane in the zeroth approximation.

introducing an image flap on the negative real axis. At large distances from the flap in the z-plane equation (8) requires that $w(z) \to -i\sqrt{z}$; in the ζ-plane the flow is uniform and parallel to the imaginary axis when $|\zeta|$ is large, and $w_0(\zeta) \to w(\zeta) \approx -i\sqrt{h}\zeta$.

The functional form of $w_0(\zeta)$ with this limiting behavior can be found by Sedov's method [27, chapter 2] to be given by

$$w_0(\zeta) = -i\sqrt{H}\int_0^\zeta \left(\sqrt{1-mt^2} - \frac{\beta}{\sqrt{1-mt^2}}\right)\frac{dt}{\sqrt{1-t^2}}, \quad \beta = \text{constant}. \tag{13}$$

The value of β is determined by the condition that the circulation about the flap should vanish, which yields

$$\beta = 1 - E(m')/K(m') > 0, \quad m' = 1 - m, \tag{14}$$

where $K(m')$, $E(m')$ are, respectively, complete elliptic integrals of the first and second kinds [28].

Higher order approximation to $w(\zeta)$ can be determined successively by imposing the condition $\mathbf{n}\cdot\nabla\varphi^* = 0$ on the flap. If $\zeta = \xi + \mathrm{i}\eta$, then correct to $O(\varepsilon)$ we must satisfy

$$\partial\varphi_1^*/\partial\eta = -\partial\varphi_0^*/\partial\xi \quad \text{for } 1 < \xi < 1/\sqrt{m}, \quad \eta = 0. \tag{15}$$

It follows from the symmetry of the problem that $\partial\varphi_0^*/\partial\xi$ is an odd function of η (which is discontinuous across $\eta = 0$ over the interval $1 < \xi < 1/\sqrt{m}$ occupied by the zeroth order flap) and therefore, from equation (15), that φ_1^* represents the field of a *monopole* source distributed over $1 < \xi < 1/\sqrt{m}$, $\eta = 0$. Accordingly, application of the method of images supplies the solution

$$w_1(\zeta) = \frac{-\sqrt{H}}{\pi}\int_1^{1/\sqrt{m}} \ln(t^2-\zeta^2)\left(\sqrt{1-mt^2} - \frac{\beta}{\sqrt{1-mt^2}}\right)\frac{\mathrm{d}t}{\sqrt{t^2-1}}, \tag{16}$$

which has zero circulation about the flap.

A more convenient representation is obtained by considering the corresponding expression for $\mathrm{d}w_1/\mathrm{d}\zeta$, obtained by differentiation of equation (16). The integral can be transformed into an integral around a closed contour in the ζ-plane that just encloses the segment $(1, 1/\sqrt{m})$ of the real axis. Cauchy's theorem permits the integral to be replaced by one along the imaginary axis together with a contribution from a simple pole at $t = \zeta$ (in $\mathrm{Re}\,\zeta > 0$), i.e.,

$$\frac{\mathrm{d}w_1}{\mathrm{d}\zeta} = \frac{2\zeta\sqrt{H}}{\pi}\int_1^{1/\sqrt{m}} \frac{(1-\beta-mt^2)}{\sqrt{t^2-1}\sqrt{1-mt^2}}\frac{\mathrm{d}t}{(t^2-\zeta^2)}$$

$$\equiv \frac{\sqrt{H}(1-\beta-m\zeta^2)}{\sqrt{1-\zeta^2}\sqrt{1-m\zeta^2}} - \frac{\zeta\sqrt{H}}{\pi}\int_{-\infty}^{\infty} \frac{(1-\beta+m\lambda^2)}{\sqrt{1+\lambda^2}\sqrt{1+m\lambda^2}}\frac{\mathrm{d}\lambda}{(\lambda^2+\zeta^2)}. \tag{17}$$

Hence, using this and equation (13), one finds

$$\frac{\mathrm{d}w}{\mathrm{d}z} \equiv \frac{\partial\varphi^*}{\partial y_1} - \mathrm{i}\frac{\partial\varphi^*}{\partial y_2} \approx \frac{\mathrm{d}w_0}{\mathrm{d}z} + \varepsilon\frac{\mathrm{d}w_1}{\mathrm{d}z}$$

$$= \frac{-\mathrm{i}[z-(1-\beta)H]}{2\sqrt{z}\sqrt{z-h}\sqrt{z-H}}\left(1+\frac{\mathrm{i}\alpha}{2}\right) - \frac{\alpha}{4\pi}\int_{-\infty}^{\infty}\frac{[\mu^2+(1-\beta)H]}{\sqrt{H+\mu^2}\sqrt{h+\mu^2}}\frac{\mathrm{d}\mu}{(\mu^2+z)}. \tag{18}$$

The real and imaginary parts of this formula determine the functional form of $\partial\varphi^*(\mathbf{y})/\partial\mathbf{y}$, which may be used in the first of equations (9) to evaluate the edge noise when the vorticity and velocity distributions, $\boldsymbol{\Omega}$ and $\mathbf{v}$, are known near the flap (e.g., from a numerical simulation of incompressible flow near the flap; cf. [14, 15]).

To calculate the sound using the second of equations (9), note first that for a thin hydrofoil it can be written in the form

$$p(\mathbf{x}, \omega) \approx \frac{\rho_0 \, \omega \sqrt{\mathrm{i}\kappa_0} \, \sin^{1/2} \psi \, \sin(\theta/2)}{\pi \sqrt{2} \, |\mathbf{x}|} \int_{S_+} [\varphi^*(\mathbf{y})] v_{In}(\mathbf{y}, \omega) \, \mathrm{e}^{|\mathbf{x} - \mathrm{i}y_3 \mathbf{i}_3|} \, \mathrm{d}S(\mathbf{y}) \quad |\mathbf{x}| \to \infty, \tag{19}$$

where the integration is over the "upper" surfaces S_+ of the hydrofoil and flap, and $[\varphi^*] = \varphi^*_+ - \varphi^*_-$ is the jump in the value of φ^* in passing from the point $\mathbf{y}$ on the lower surface to the corresponding point on the upper surface. $[\varphi^*]$ can be determined by integrating the jump $\mathrm{d}[w]/\mathrm{d}z$ defined by equation (18). Introducing the approximation $1 + \mathrm{i}\alpha/2 \approx \mathrm{e}^{\mathrm{i}\alpha/2}$, one finds

$$[\varphi^*] = 2 \sqrt{\frac{|y_1|(H - y_1)}{h - y_1}} - 2H^{1/2} \{\mathscr{E}(\tan^{-1}(\sqrt{|y_1|/h}), m') - (1 - \beta)\mathscr{F}(\tan^{-1}(\sqrt{|y_1|/h}), m')\}, \quad y_1 < 0 \text{ on the hydrofoil}, \tag{20}$$

$$[\varphi^*] = 2 \sqrt{\frac{(H - y_\parallel)(y_\parallel - h)}{y_\parallel}} - 2H^{1/2} \{\mathscr{E}(\sin^{-1}(\sqrt{H(y_\parallel - h)/y_\parallel l}), m') - (1 - \beta)\mathscr{F}(\sin^{-1}(\sqrt{H(y_\parallel - h)/y_\parallel l}), m')\}, \quad h < y_\parallel < H \text{ on the flap}, \tag{21}$$

where

$$\mathscr{E}(\xi, m') = \int_0^\xi \sqrt{1 - m' \sin^2 \mu} \, \mathrm{d}\mu, \quad \mathscr{F}(\xi, m') = \int_0^\xi \frac{\mathrm{d}\mu}{\sqrt{1 - m' \sin^2 \mu}} \tag{22}$$

and $y_\parallel$ denotes the distance measured parallel to the surface of the flap (i.e., in a direction inclined at the flap angle α) from the edge O of the hydrofoil.

3.2. CRITICAL BEHAVIOR NEAR THE EDGES OF THE FLAP AND HYDROFOIL

The solid curves in Figure 3 represent the potential flow streamlines $\psi_0^* = \text{constant}$ for the zeroth approximation $w_0 = \varphi_0^* + \mathrm{i}\psi_0^*$ when $l = 4h$ ($m = 0{\cdot}2$), calculated from equation (13) by setting $\zeta = \sqrt{z/h}$. The volume flux between neighboring streamlines is the same in all cases; thus convergence of the streamlines near the leading and trailing edges of the slot between the hydrofoil and flap, and near the trailing edge of the flap correspond to regions where $\mathbf{\nabla}\varphi_0^*$ is large and where, according to equation (9), the efficiency of edge scattering of turbulence sources becomes large. The stagnation streamline intersects the flap symmetrically and is indicated by the broken line curve in the figure.

The behaviors of $\varphi^*(\mathbf{y}) \equiv \mathrm{Re}\, w(\zeta)$ near the edges of the flap and hydrofoil are determined by expanding $w(\zeta) \equiv w(\sqrt{z/h})$ about the critical points at $z = 0$, h, $H(= l + h)$. To the present order-ε approximation, the singularities at $z = 0$, h, and H occur, respectively, at the edge of the hydrofoil, and at the leading and trailing edges of the flap. By expanding the second line of equation (18) about each of these points and integrating with respect to z we

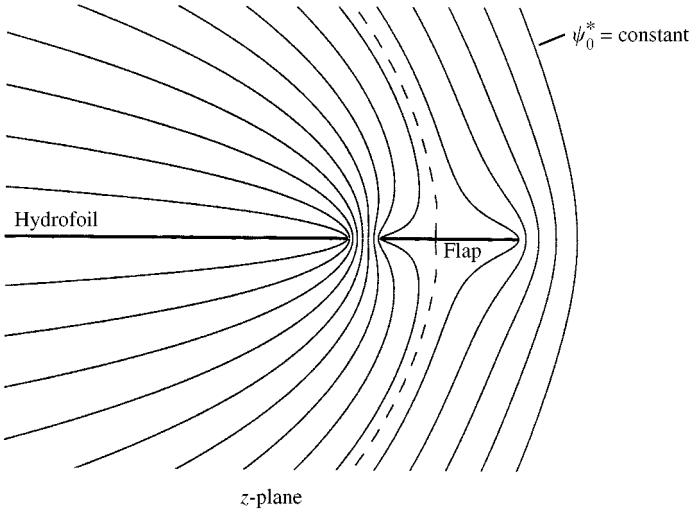

Figure 3. Streamlines $\psi_0^* = \text{constant}$ in the z plane for the zeroth order approximation $w_0 = \varphi_0^* + \mathrm{i}\psi_0^*$ when $l = 4h$.

find (after discarding irrelevent constants of integration)

$$\text{hydrofoil trailing edge:} \qquad w \sim -\mathrm{i}\sqrt{z}\,(1-\beta)\sqrt{1+\frac{l}{h}},$$

$$\text{flap leading edge:} \qquad w \sim \sqrt{z-h}\,\mathrm{e}^{\mathrm{i}\alpha/2}\left[(1-\beta)\left(1+\frac{l}{h}\right)-1\right]\sqrt{\frac{h}{l}},$$

$$\text{flap trailing edge:} \qquad w \sim -\mathrm{i}\sqrt{z-(h+l)}\,\mathrm{e}^{\mathrm{i}\alpha/2}\,\beta\sqrt{1+\frac{h}{l}}. \tag{23}$$

The corresponding approximations for $\varphi^*(\mathbf{y}) = \mathrm{Re}\, w$ can be written

$$\text{hydrofoil trailing edge:} \qquad \varphi^* \sim -\sqrt{r_\mathrm{O}}\sin\left(\frac{\theta_\mathrm{O}}{2}\right)(1-\beta)\sqrt{1+\frac{l}{h}},$$

$$\text{flap leading edge:} \qquad \varphi^* \sim \sqrt{r_h}\cos\left(\frac{\theta_h+\alpha}{2}\right)\left[(1-\beta)\left(1+\frac{l}{h}\right)-1\right]\sqrt{\frac{h}{l}},$$

$$\text{flap trailing edge:} \qquad \varphi^* \sim \sqrt{r_H}\sin\left(\frac{\theta_H+\alpha}{2}\right)\beta\sqrt{1+\frac{h}{l}}, \tag{24}$$

where (r_O, θ_O), (r_h, θ_h), (r_H, θ_H) are, respectively, the polar co-ordinates of the source point (y_1, y_2) relative to the edge O of the hydrofoil, to the flap leading edge, and the flap trailing edge.

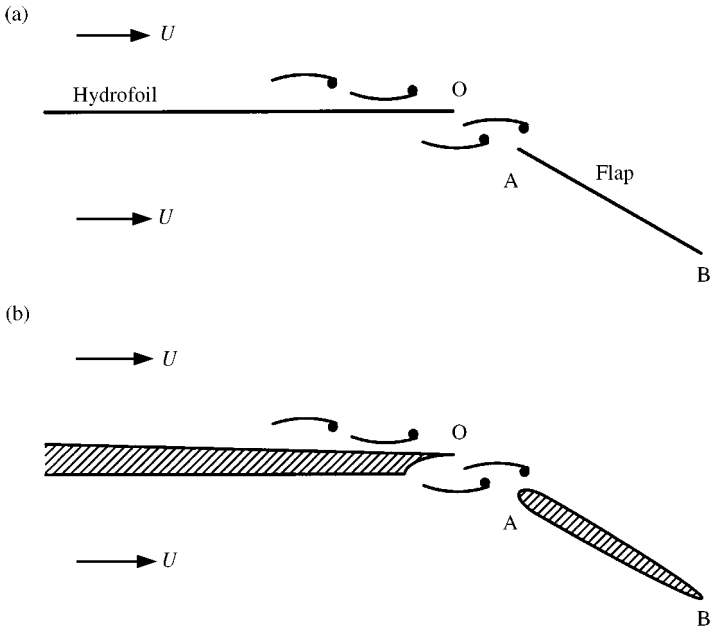

Figure 4. (a) Turbulence interacting with the hydrofoil and flap; (b) generalized trailing edge configuration.

4. COMMENTS ON TRAILING EDGE AND FLAP GENERATED SOUND

4.1. TRAILING EDGE NOISE

An important component of the sound generated by the trailing edge region can be attributed to turbulence whose characteristic length scale is small compared to the flap chord l. In this case, the effective acoustic sources at the edges labelled O, A and B in Figure 4(a) will be statistically independent, and their relative contributions to the farfield sound can be estimated by inserting the corresponding approximations (24) for $\varphi^*(\mathbf{y})$ into the second of equations (9) and performing local surface integrations.

The upwash velocity $\mathbf{v}_I$ is produced by the turbulence convecting past the edges, augmented by the induced velocity of any additional vorticity shed from the trailing edges (to satisfy the unsteady *Kutta condition* [29]). The effect of this shedding is to greatly reduce the importance of the edges O and B as sources of sound, because the induced velocity of the shed vorticity acts to oppose that produced by impinging turbulence. This does not occur at the leading edge A: provided the flow does not separate near A, any vorticity generated there is swept downstream over the surface of the flap, and its induced velocity is therefore cancelled by an equal and opposite velocity produced by image vertices in the flap. Thus, impingement noise generated at A is likely to be the principal source of sound in the trailing edge region.

However, it is possible for the trailing edges O and B to remain significant sources of *high-frequency* sound. It follows from equation (9) by inserting the corresponding local approximation of $\varphi^*(\mathbf{y})$ from equation (24), that the relative *intensities* of the corresponding acoustic pressures p_O, p_B, say, satisfy

$$\left(\frac{p_O}{p_B}\right)^2 \sim \left(\frac{v_O}{v_B}\right)^2 \frac{l}{h}\frac{(1-\beta)^2}{\beta^2}, \tag{25}$$

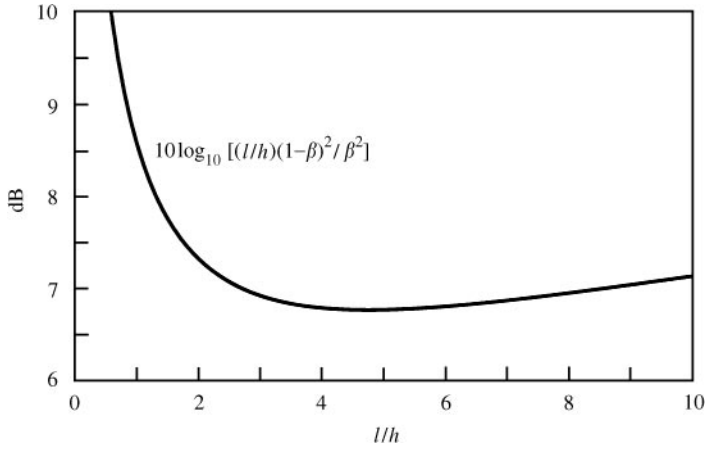

Figure 5. Relative efficiency of trailing edge noise generation at O and B in Figure 4.

where v_O, v_B are characteristic turbulence velocities (e.g., friction velocities), respectively, near the trailing edge of the trailing edges of the hydrofoil and flap. The relative *efficiency* factor. $10\log_{10}[(l/h)(1-\beta)^2/\beta^2]$ (dB) determines the ratio of the intensities of the sound produced at O and B when the magnitudes of the turbulence velocities are nominally equal; it is plotted as a function of l/h in Figure 5, from which it is seen that the efficiency of edge noise production at the trailing edge O of the hydrofoil exceeds that at the trailing edge of the flap typically by 7 dB or more. To understand this, one might note that the relatively high acoustic efficiency of traditional trailing edge noise (proportional to the Mach number M) is attributed to the presence of the adjacent, acoustically non-compact surface of the hydrofoil; for the edge noise produced by the flap, however, the influence of non-compactness is "short circuited" by the presence of the slot, to an extent at least equivalent to a reduction in efficiency of 7 dB.

4.2. EQUIVALENT FLAP-IMPINGEMENT NOISE DIPOLE

Equations (9) and the second of equation (24) show that the acoustic pressure generated by small-scale turbulence impinging on the leading edge of the flap at A is given by

$$p(\mathbf{x},\omega) \sim \frac{f\rho_0\omega\sqrt{2\mathrm{i}\kappa_0}\,\sin^{1/2}\psi\,\sin(\theta/2)\mathrm{e}^{\mathrm{i}\kappa_0|\mathbf{x}|}}{\pi^{3/2}\,|\mathbf{x}|}$$

$$\times\int_{-\infty}^{\infty}\mathrm{d}y_3\int_h^{l+h}\sqrt{y_\parallel-h}\,v_\perp(y_\parallel,y_3,\omega)\,\mathrm{e}^{-\mathrm{i}\kappa_0\cos\psi y_3}\,\mathrm{d}y_\parallel \quad |\mathbf{x}|\to\infty, \qquad (26)$$

where $v_\perp(y_\parallel, y_3, \omega)$ is the normal component of the upwash velocity (directed "upwards" from the flap), expressed in terms of the distance $y_\parallel$ measured along the flap from A, and

$$f \equiv f(l/h) = \sqrt{h/l}\,[(1-\beta)(1+l/h)-1]. \qquad (27)$$

The turbulence impinging on the leading edge A produces lift fluctuations on the flap. The magnitude of this lift force will be influenced to some extent by the proximity of the

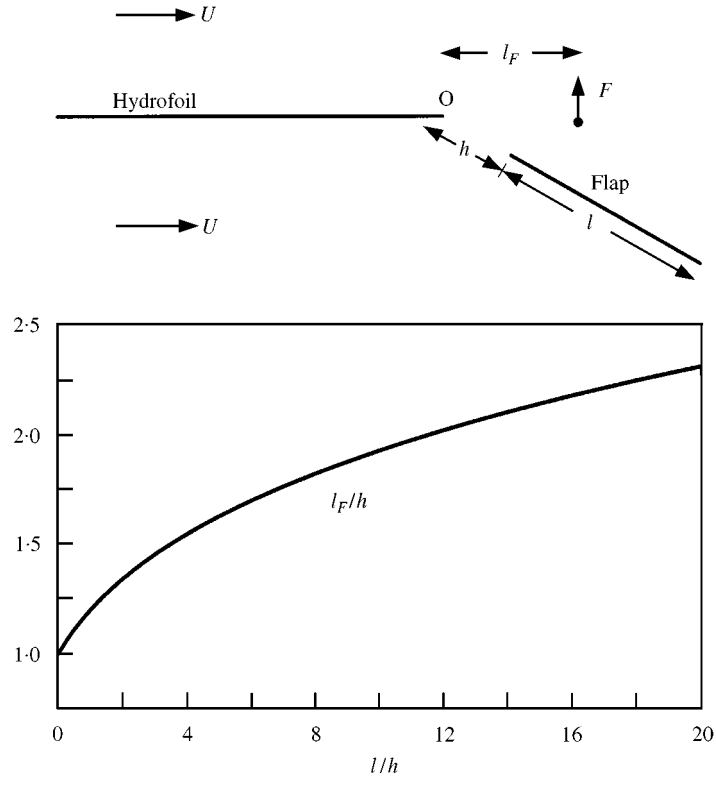

Figure 6. Line of action of equivalent dipole lift force F for calculating flap leading-edge-impingement noise.

hydrofoil, but for small-scale turbulence the influence will be small, and the force will be close to its value when the hydrofoil is absent, because it is dominated by interactions between the turbulence and the flap taking place in the immediate vicinity of the noise. The lift per unit span at frequency ω for a thin-plate flap, when the reduced frequency $\omega l/U > 1$, and when the influence of the main hydrofoil is ignored, is given by [2, 30]

$$F(y_3, \omega) = -2\mathrm{i}\rho_0\omega\sqrt{l}\int_h^{l+h}\sqrt{y_\parallel - h}\, v_\perp(y_\parallel, y_3, \omega)\,\mathrm{d}y_\parallel. \tag{28}$$

This is equivalent to the classical Sears formula [31] when $v_\perp(y_\parallel, y_3, \omega)$ is assumed *not* to depend on the spanwise co-ordinate y_3.

Let us determine the sound generated by this force when it is regarded as distributed along a spanwise line at distance l_F to the rear of the hydrofoil *in the absence of a flap* (see Figure 6). The force on the fluid is $(0, -F, 0)$ and the acoustic pressure is therefore determined by [2]

$$(\nabla^2 + \kappa_o^2)p = -(\partial/\partial x_2)\,(\delta(x_1 - l_F)\delta(x_2)F(x_3, \omega)) \tag{29}$$

subject to $\partial p/\partial x_2 = 0$ on the hydrofoil. The solution can be expressed in terms of the component $G_1(\mathbf{x}, \mathbf{y}, \omega)$ of the Green function (6), where (because the flap is now absent and

represented by F) $\varphi^*(\mathbf{y})$ is given its limiting form in equation (8):

$$p(\mathbf{x},\omega) = -\int G_1(\mathbf{x},\mathbf{y},\omega)\frac{\partial}{\partial y_2}(\delta(y_1 - l_F)\delta(y_2)F(y_3,\omega))\,\mathrm{d}^3\mathbf{y}$$

$$= \frac{-\sqrt{\kappa_0}\sin^{1/2}\psi\sin(\theta/2)\mathrm{e}^{\mathrm{i}\kappa_0|\mathbf{x}|}}{2\pi\sqrt{2\pi}\,\mathrm{i}l_F|\mathbf{x}|}\int_{-\infty}^{\infty} F(y_3,\omega)\,\mathrm{e}^{-\mathrm{i}\kappa_0\cos\psi y_3}\,\mathrm{d}y_3$$

$$= \sqrt{\frac{l}{4l_F}}\frac{\rho_0\omega\sqrt{2\mathrm{i}\kappa_0}\sin^{1/2}\psi\sin(\theta/2)\,\mathrm{e}^{\mathrm{i}\kappa_0|\mathbf{x}|}}{\pi^{3/2}|\mathbf{x}|}$$

$$\times\int_{-\infty}^{\infty}\mathrm{d}y_3\int_h^{l+h}\sqrt{y_\parallel - h}\,v_\perp(y_\parallel,y_3,\omega)\,\mathrm{e}^{-\mathrm{i}\kappa_0\cos\psi y_3}\,\mathrm{d}y_\parallel \quad |\mathbf{x}|\to\infty. \tag{30}$$

This will coincide with the directly calculated radiation (26) if $l_F = l/4f^2$. In other words, they are equal when the dipole F is situated downstream of the hydrofoil trailing edge O *in the absence of the flap* at a distance given by

$$\frac{l_F}{h} = \frac{(l/h)^2}{4[(1-\beta)(1+l/h)-1]^2}. \tag{31}$$

This function is plotted in Figure 6. Evidently, l_F/h increases very slowly as the chord of the flap increases (ultimately proportional to $[\ln(16l/h)/4]^2$), and l_F does not exceed twice the slot width h until $l/h > 12$.

When the statistical properties of $F(y_3,\omega)$ are known the frequency spectrum $\Phi(\mathbf{x},\omega)$ of the acoustic pressure at $\mathbf{x}$ (which satisfies $\langle p^2(\mathbf{x},t)\rangle = \int_{-\infty}^{\infty}\Phi(\mathbf{x},\omega)\,\mathrm{d}\omega$, where $\langle\ \rangle$ denotes an ensemble average) is readily calculated. For stationary random turbulence

$$\langle F(y_3,\omega)F^*(y_3',\omega')\rangle = \delta(\omega-\omega')\Phi_{FF}(\omega)\mathscr{R}(|y_3 - y_3'|,\omega), \tag{32}$$

where $\Phi_{FF}(\omega)$ is the frequency spectrum of the lift per unit span (defined such that $\langle|F(y_3,\omega)|^2\rangle = \int_{-\infty}^{\infty}\Phi_{FF}(\omega)\,\mathrm{d}\omega$), and $\mathscr{R}(y,\omega)$ is the corresponding spanwise covariance (for which $\mathscr{R}(0,\omega)=1$).

In terms of these definitions, it is easily deduced from the second of equations (30) that

$$\Phi(\mathbf{x},\omega) \approx \frac{\sin\psi\sin^2(\theta/2)}{(2\pi)^3|\mathbf{x}|^2}\frac{Ll_3}{c_0 l_F}\omega\Phi_{FF}(\omega) \quad |\mathbf{x}|\to\infty, \tag{33}$$

where $l_3 = \int_{-\infty}^{\infty}\mathscr{R}(y,\omega)\,\mathrm{d}y$ is the spanwise correlation length of the lift and $L \gg l_3$ is the span of the flap wetted by the turbulent flow. The spanwise correlation scale is frequency dependent, and typically $l_3 \sim U/\omega$, so that $\kappa_0 l_3 \sim M \ll 1$; this condition has been used in deriving equation (33). The order of magnitude of the flap mean-square acoustic pressure is

$$\langle p^2\rangle \sim \mathscr{C}\,(l/|\mathbf{x}|)^2\,(L/l_F)\,(\rho_0 U^2)^2 M, \tag{34}$$

where typically $\mathscr{C} \sim 10^{-2} \sim$ mean-square turbulence velocity/U^2 [32]. This is characteristic of overall edge generated sound when the hydrofoil chord is large compared to the acoustic wavelength, and the flap may therefore be regarded as augmenting the usual trailing edge noise, without changing the overall efficiency or directivity, although perhaps extending the spectrum to encompass the lower frequencies that are more preferentially generated at the flap leading edge.

4.3. HYDROFOIL AND FLAP OF FINITE THICKNESS

These detailed conclusions for small-scale turbulence sources are applicable to the more general trailing edge configuration sketched in Figure 4(b). Formulae (24) for $\varphi^*(\mathbf{y})$ now constitute "outer approximations" to the potential function defining irrotational flow around the trailing edge region. $\varphi^*(\mathbf{y})$ varies in a more complicated manner close to the rounded edges of the flap, or near the thickened geometry of the hydrofoil trailing edge, but will tend to the forms given in equation (24) when the distance from an edge exceeds the edge radius of curvature. This indicates that the above predictions of, say, the flap impingement noise should still be valid for components of the upwash velocity whose length scales are larger than the leading edge radius of curvature of the flap. But these would be expected to be the dominant small-scale noise sources, since the efficiency of sound generation, which depends on "scattering" by surface irregularities, tends to fall off rapidly when the turbulence scale becomes smaller than the radius of curvature [2]. In particular, the result in Figure 6 for the location of the effective flap dipole source should remain true for the dominant turbulence sources.

5. CONCLUSION

The sound produced by a trailing edge with a detached flap has three principal sources. First, there is the "self-noise" attributed to small-scale turbulence produced by instabilities in the boundary layers upstream of the hydrofoil and flap trailing edges. This is of relatively high frequency, because the sound that would be generated by larger scale turbulence eddies (large on a scale of hydrofoil or flap thickness near the edge) tends to be cancelled by that produced by vorticity shed from the edge in accordance with the Kutta condition. Second, impingement noise is produced when turbulence is swept past the leading edge of the flap, creating an unsteady lift force that generates sound by interaction with the trailing edge of the hydrofoil. Finally, the side edges of part-span flaps constitute important sources of lower frequency noise, associated with the interaction of side-edge lift vortices with the side-and trailing edge.

The formulae given in this paper for the compact Green function for a trailing edge with a single detached flap can be used to predict the trailing edge self-noise and the flap impingement noise in flows at low Mach number. To do this it is first necessary to determine the unsteady velocity and vorticity distributions in the vicinity of the flap, or the equivalent upwash velocity produced by the unsteady flow.

The analytical results for a flap at a modest angle of attack α (where $\alpha^2 \ll 1$) indicate, that the self-noise produced at the edge of the hydrofoil is typically at least 7 dB in excess of that produced at the flap trailing edge. The strength of the noise generated by impingement of small-scale turbulence on the flap leading edge can be calculated by first determining the unsteady lift $F(\omega)$ per unit span produced by the turbulence when the flap is regarded as an *isolated hydrofoil*, for example, by means of a convenient "strip-theory" approximation

based on Sears' formula for the lift produced by a gust. The radiation is then equal to that produced by a dipole of strength—F situated at distance l_F to the rear of the edge of the main hydrofoil; this distance is given as a function of flap dimensions by equation (27). The dipole radiation intensity is increased from its classical free-field value by the proximity of the hydrofoil trailing edge, typically by a factor $\sim O(1/M)$ ($\gg 1$); similarly its directly is modified by the presence of the hydrofoil, so that the peak radiation occurs in "forward" directions (near $\theta = \pm 180^\circ$).

In this paper, it has been assumed that the hydrofoil chord is much larger than all other length scales, including the acoustic wavelength. This condition can be relaxed, however (provided the characteristic acoustic wavelength remains large compared to the flap chord), without changing the principal conclusions, by introducing the frequency-dependent correction factor given in reference [16] for dealing with hydrofoils of finite chord. Predictions of this paper can therefore be used to validate acoustic numerical schemes applied to a finite chord hydrofoil with a detached flap of suitably simple geometry. Similarly, general formula (9) for the edge generated sound is also applicable to more realistic flap and hydrofoil geometries; in such cases, however, the potential function $\varphi^*(y)$ would need to be determined numerically.

ACKNOWLEDGMENTS

The work reported in this paper was supported by the Office of Naval Research under Grant N00014-99-1-0391 administered by Dr L. Patrick Purtell. The author gratefully acknowledges the benefit of discussions with Dr William K. Blake.

REFERENCES

1. N. CURLE 1955 *Proceedings of the Royal Society* **A 231**, 505–514. The influence of solid boundaries upon aerodynamic sound.
2. M. S. HOWE 1998 *Acoustics of Fluid–Structure Interactions*. Cambridge: Cambridge University Press.
3. J. E. FFOWCS WILLIAMS and D. L. HAWKINGS 1969 *Philosophical Transactions of the Royal Society* **A 264**, 321–342. Sound generation by turbulence and surfaces in arbitrary motion.
4. J. C. HARDIN and J. E. MARTIN 1997 *American Institute of Aeronautics and Astronautics Journal* **35**, 810–815. Flap side-edge noise: acoustic analysis of Sen's model.
5. M. S. HOWE 1999 *Journal of Sound and Vibration* **225**, 211–238. Trailing edge noise at low Mach numbers.
6. D. M. CHASE 1972 *Journal of the Acoustical Society of America* **52**, 1011–1023. Sound radiated by turbulent flow off a rigid half-plane as obtained from a wavevector spectrum of hydrodynamic pressure.
7. K. L. CHANDIRAMANI 1974 *Journal of the Acoustical Society of America* **55**, 19–29. Diffraction of evanescent waves, with applications to aerodynamically scattered sound and radiation from unbaffled plates.
8. D. M. CHASE 1975 *American Institute of Aeronautics and Astronautics Journal* **13**, 1041–1047. Noise radiated from an edge in turbulent flow.
9. M. J. LIGHTHILL 1952 *Proceedings of the Royal Society* **A 211**, 564–587. On sound generated aerodynamically. Part I: general theory.
10. M. J. LIGHTHILL 1954 *Proceedings of the Royal Society* **A 222**, 1–32. On sound generated aerodynamically. Part II: turbulence as a source of sound.
11. J. E. FFOWCS WILLIAMS and L. H. HALL 1970 *Journal of Fluid Mechanics* **40**, 657–670. Aerodynamic sound generation by turbulent flow in the vicinity of a scattering half-plane.
12. P. E. DOAK 1960 *Proceedings of the Royal Society* **A 254**, 129–145. Acoustic radiation from a turbulent fluid containing foreign bodies.

13. M. WANG 1997 *Annual Research Briefs*, 37–49. *Center for Turbulence Research Stanford University*. Progress in large-eddy simulation of trailing-edge turbulence and aeroacoustics.
14. M. WANG 1998 *Annual Research Briefs*, 91–106, *Center for Turbulence Research*, *Stanford University*. Computation of trailing-edge noise at low mach number using LES and acoustic analogy.
15. M. WANG and P. MOIN 1999 *American Institute of Aeronautics and Astronautics Journal*. Computation of trailing-edge noise using large-eddy simulation (in press).
16. M. S. HOWE 1999 *Quarterly Journal of Mechanics and Applied Mathematics*. Edge-source acoustic Green's function for an airfoil of arbitrary chord, with application to trailing edge noise (in press).
17. T. Z. DONG, C. K. W. TAM and N. N. REDDY 1999 *AIAA Paper* 99-1803. Direct numerical simulation of flap side edge noise.
18. T. H. WOOD and S. M. GRACE 1999 *AIAA Paper* 99-1893. Aeroacoustic predictions of a wing-flap configuration in three dimensions.
19. T. H. WOOD and S. M. GRACE 2000 *AIAA Paper* 0607. Free-wake analysis for calculating the aeroacoustics of a wing-flap configuration.
20. Y. P. GUO 1997 *AIAA Paper* 97-1647. A model for slat-noise generation.
21. M. S. HOWE 1982 *Journal of Sound and Vibration* **80**, 555–573. On the generation of side-edge flap noise.
22. M. S. HOWE 1998 *Boston University*, *Department of Aerospace and Mechanical Engineering*. *Report AM*-98-001, Reference manual on the theory of lifting surface noise at low Mach numbers.
23. M. S. HOWE 1978 *Aeronautical Research Council Reports & Memoranda No*. 3830. The generation of sound by a slot in an aerofoil.
24. M. S. HOWE 1980 *Proceedings of the Royal Society* **A 373**, 253–272. Aerodynamic sound generated by a slotted trailing edge.
25. HORACE LAMB 1932 *Hydrodynamics*. Cambridge: Cambridge University Press (Reprinted 1993), sixth edition.
26. G. K. BATCHELOR 1967 *An Introduction to Fluid Dynamics*. Cambridge: Cambridge University Press.
27. L. I. SEDOV 1965 *Two Dimensional Problems in Hydrodynamics and Aerodynamics*. New York: John Wiley.
28. M. ABRAMOWITZ and I. A. STEGUN (editors) 1970 *Handbook of Mathematical Functions* (ninth corrected printing). U.S. Department of Commerce, National Bureau of Standards Applied Mathematics Series No. 55.
29. D. G. CRIGHTON 1985 *Annual Reviews of Fluid Mechanics* **17**, 411–445. The Kutta condition in unsteady flow.
30. M. S. HOWE 1999 *Journal of Fluids and Structures*. Unsteady lift and sound produced by an airfoil in a turbulent boundary layer (in press).
31. W. R. SEARS 1941 *Journal of the Aeronautical Sciences* **8**, 104–108. Some aspects of non-stationary airfoil theory and its practical applications.
32. J. O. HINZE 1975 *Turbulence* New York: McGraw-Hill, second edition.